Temperature Dependence of Radiative Association Rates

Victor Ryzhov, Yu-Chuan Yang,† Stephen J. Klippenstein,* and Robert C. Dunbar*

Department of Chemistry, Case Western Reserve University, Cleveland, Ohio 44106

Received: March 6, 1998; In Final Form: June 29, 1998

The formation of gas-phase complexes by radiative association is a strongly temperature-dependent process, whose modeling provides a good test of theoretical approaches to modeling the kinetics and whose predictability is useful for temperature extrapolations. The temperature dependence of the low-pressure association rate constants, measured in the Fourier transform ion cyclotron resonance mass spectrometer, was considered for four systems, acetone/(acetone)H^+, acetone-d_6/(acetone-d_6)D^+, butanone/(butanone)H^+, and NO^+/3-pentanone. For the first two systems, the experimentally measured temperature range was extended down to 245 K to complement data already available for room and higher temperatures. The data for the third system above room temperature are new, while data for the final system, already available from our earlier experiments, are reconsidered here. Modeling was done by variational transition-state theory (VTST), incorporating ab initio calculations of vibrational frequencies and infrared emission intensities. The VTST-based approach gave excellent agreement with the measured values of the rate constants and their temperature dependences. The results suggest that VTST-based modeling provides an adequate description of the radiative association kinetics and can serve as an accurate approach for making binding energy estimates from experimental association results.

Introduction

In low-pressure environments such as are found in deep space or in high-vacuum ion-trapping laboratory instruments, one of the most important chemical reaction paths available to ionic molecules is radiative association.[1−8] In this process, the combination of a gas-phase ion with a neutral molecule forms a stable complex when the metastable collision complex disposes of some of its initial internal excitation by photon emission, usually in the infrared spectral region. The rates of these reactions exhibit a very strong temperature dependence. The temperature dependence is not described by any simple, transparent relation, and modeling it accurately is a good test of the validity of the theoretical understanding of the kinetics. Recently, theoretical approaches to this kinetic modeling have advanced to a point of considerable confidence, and the present study combines these approaches with old and new data for several representative systems to show the excellent agreement which can now be hoped for between theory and experiment. Several recent reviews have discussed the kinetics of radiative association reactions and describe both the theoretical and observational state of understanding of this chemistry.[1,6,9]

Kinetic analysis of radiative association observations (the RA kinetics approach) can be a useful tool for quantitative estimations of the binding energy of complexes.[10−16] Full-scale applications of RA kinetics analysis using VTST-based modeling drawing on ab initio calculations[12,13] have been repaid with binding energy values of precision comparable to alternative techniques and have given us some confidence in the validity and utility of this approach. For this purpose, it is desirable to observe the kinetics in the region of temperature where the reaction is neither too fast (near collisional efficiency) nor too slow (less than about 0.1% efficient). This generally constrains the temperature fairly severely and means that different reactions will present observational information at different temperatures. It is accordingly essential to have confidence in our ability to extrapolate kinetic parameters from the observationally convenient temperature range into the temperature range where comparisons are to be made and also to have confidence that data analyses for different reactions at different temperatures are equally valid.

The first system chosen for temperature dependence study was acetone/protonated acetone, for which the experimental data are particularly abundant and deserving of confidence. The association rate in this system at room temperature is well-known thanks to work by McMahon et al.[2,17,18] and Ridge et al.[19]; substantial data on temperature dependence are available from these sources. Using the same ion−molecule reaction for pressure calibration as McMahon,[2,18] we obtained a very similar value of the rate constant. This allowed us to compare our results directly with theirs. For acetone-d_6/deuteronated acetone-d_6 it was possible to combine data from McMahon's group[18] with our more extensive data and with already completed ab initio calculations from our earlier work.[13] Butanone/protonated butanone was a convenient system for careful temperature dependence study, following our previous work on the kinetics at room temperature.[20] The association efficiency in this system is in a convenient range, far away from the collisional limit but still high enough to permit study over a usefully wide temperature range. Binding energies in these systems are well-known, 30.6 kcal mol^{-1} for acetone/protonated acetone,[21] 30.6 kcal mol^{-1} for butanone/protonated butanone,[21] and 41.6 kcal mol^{-1} for NO^+/3-pentanone.[16]

It also seemed appropriate to compare our new results with our earlier work on temperature dependence in the NO^+/3-pentanone system.[16]

* To whom correspondence should be addressed.

† Present address: Chemistry Department, University of Maryland, Baltimore Co., Baltimore, MD.

10.1021/jp9814092 CCC: $15.00
Published on Web 10/16/1998

Experimental Section

Experiments were performed on an FT-ICR spectrometer with a 2.54-cm cubical cell. The details of the instrument were described elsewhere.[22,23] Neutrals were introduced into the cell through leak valves (Varian). NO was ionized by electron impact (electron energy 15 eV). Protonated acetone and butanone as well as deuteronated acetone-d_6 ions were formed by self-CI after electron-impact ionization of the neutrals. The pressure of the neutrals varied from 5×10^{-9} to 5×10^{-6} Torr. The ion gauge pressure readings were calibrated to match the known proton-transfer rate constant between acetyl cation and acetone[18] for acetone, acetone-d_6, and butanone experiments. After ion formation, a thermalization period allowing at least five ion-neutral collisions was provided. Then the desired ions were isolated by a series of ejection pulses and allowed to react for a time which ranged from 200 ms to 20 s, after which the extent of association was measured as a function of the reaction time. To avoid cell heating by the hot filament, the filament was turned off before the thermalization period (a pulsed filament mode), as has been described for other studies in our laboratory where temperature equilibration of the cell at ambient temperature was vital.[10,23,24] An idle time of up to 20 s was provided in each working cycle so that the filament on time was less than 10%.

For high-temperature experiments, the reaction chamber was heated by surrounding it with heating tapes and insulation. The cell temperature was monitored by a copper−constantan thermocouple located on the trapping plate of the ICR cell. For low-temperature association measurements, the vacuum can was cooled by immersion in a dry ice/methanol bath. The cell temperature reached a steady value of 245 K, as monitored by the thermocouple.

Modeling Details

An association reaction can be analyzed in terms of the detailed mechanism

$$A^+ + B \underset{k_b}{\overset{k_f}{\rightleftharpoons}} A^+B^* \xrightarrow{k_r} A^+B \qquad (1)$$

$$A^+B^* \xrightarrow{[M],\ k_c\beta} A^+B$$

where k_f is the bimolecular rate constant for collisional complex formation,[25] k_b is the unimolecular redissociation rate constant, k_r is the unimolecular rate constant for IR photon emission from the energized complex, and $k_c\beta$ is the bimolecular rate constant for collisional stabilization of A^+B^* by collision with neutral M. A^+B^* is the metastable collision complex. At low pressures where three-body collisional stabilization of the complex is negligible, the overall bimolecular rate constant k_2 can be renamed k_{ra}, the bimolecular rate constant for radiative association, and the kinetics simplifies to give

$$k_2(\text{low pressure}) = k_{ra} = k_f k_r/(k_b + k_r) \qquad (2)$$

All of the microscopic rate constants appearing here depend on temperature. While k_f and k_r display only weak temperature dependences, k_b is highly temperature-sensitive. The rate constant k_f can be readily estimated, using the dipole-corrected Langevin equation.[9,25] The rate constants k_r and k_b are not easily estimated, and modeling them demands the resources of fairly good theoretical approaches.

Because k_f, k_r, and k_b correspond to reactions having species in common, the transition-state theory calculation of the overall rate constant k_{ra} benefits from some cancellation of common factors, as seen below (eq 5). In the limit of low association efficiency per collision, this cancellation leads to the convenient disappearance of all of the properties of the transition state from the calculation.

TABLE 1: Reactant−Molecule Vibrational Frequencies for Formation of Butanone Protonated Dimer, HF/6-31G* Calculations[a]

molecule	frequency (cm^{-1})
$CH_3C(OH)CH_2CH_3^+$	64.6, 121, 217, 238, 417, 532, 612, 815, 843, 877, 998, 1071, 1085, 1185, 1221, 1259, 1364, 1437, 1517, 1548, 1568, 1583, 1613, 1627, 1633, 1652, 1753, 3197, 3236, 3241, 3295, 3300, 3320, 3332, 3354, 3954
$CH_3COCH_2CH_3$	53.1, 120, 236, 272, 432, 557, 624, 805, 854, 1020, 1060, 1081, 1203, 1240, 1345, 1410, 1488, 1550, 1564, 1613, 1616, 1630, 1647, 1651, 2014, 3202, 3209, 3213, 3267, 3270, 3279, 3291, 3321

[a] Frequencies given here are unscaled but were scaled downward by 0.89 for use in the kinetics calculations.

Variational transition-state theory (VTST)-based modeling along with ab initio calculations of IR frequencies and intensities have given excellent results in terms of calculating and combining these rate constants to predict accurate kinetics.[12,13] The VTST-based approach has been described in detail previously;[12,13] in addition, the recent books of Gilbert and Smith [26] and Baer and Hase[27] give useful introductions to some of the kinetics issues and approaches involved. The calculation of k_{ra} consists of the following two major parts:

The first part is the calculation of the radiative rate constant, k_r, giving the rate of emission of IR photons. In the harmonic approximation, the IR photon emission rate constant for a distribution of vibrational states is given by

$$k_r(s^{-1}) = \sum_{n=1}^{N}\sum_{i=1}^{N} 1.25 \times 10^{-7}\, nP_i(n)I_i(n)\nu^2 \qquad (3)$$

where N is the number of vibrational modes, $P_i(n)$ is the probability of mode i being in level n, I_i (km mol^{-1}) is the IR absorption intensity for the $0 \rightarrow 1$ transition of mode i, and υ_i (cm^{-1}) is the ith vibrational frequency. The probability $P_i(n)$ can be calculated by a state-counting algorithm,[28] or it can be written with high accuracy from a canonical distribution

$$P_i(n) = \frac{e^{-\epsilon_i(n)/kT}}{\sum_{n=1}^{N} e^{-\epsilon_i(n)/kT}} \qquad (4)$$

where $\epsilon_i(n)$ is the energy of the nth level of the ith mode and T is the effective internal temperature of the ion.[29]

Individual IR absorption intensities and vibrational frequencies were calculated ab initio for each complex AB^+ using GAUSSIAN 94 software.[30] For the butanone system, Hartree−Fock (HF) calculations with the 6-31G* basis set were used. For the acetone systems, it was feasible to improve this level of calculation with correlation corrections via Möller−Plesset perturbation theory (MP2). All geometries were optimized at the same level of calculation as was used for the frequency/intensity evaluation. Values of frequencies and intensities from these calculations not previously published are given in Tables 1−4. By inspecting the effect of the MP2 correlation correction on the acetone results, it is seen that the vibrational frequencies are not strongly affected but that the IR intensities of the

TABLE 2: Reactant−Molecule Vibrational Frequencies for Formation of Acetone-d_6 Deuteronated Dimer, MP2/6-31G* Calculations[a]

molecule	frequency (cm^{-1})
$CD_3C(OD)CD_3^+$	69.4, 85.2, 336, 401, 453, 562, 731, 765, 778, 886, 939, 1003, 1060, 1064, 1072, 1083, 1118, 1170, 1431, 1624, 2222, 2228, 2348, 2351, 2397, 2416, 2611
CD_3COCD_3	42.9, 105, 323, 410, 485, 699, 721, 743, 920, 1007, 1057, 1101, 1106, 1107, 1116, 1145, 1309, 1781, 2232, 2235, 2357, 2362, 2399, 2401

[a] Frequencies given here are unscaled but were scaled downward by 0.95 for use in the kinetics calculations.

TABLE 3: Complex-Ion Vibrational Frequencies, Intensities, and Rotational Constants for $(CH_3COCH_2CH_3)_2H^+$, HF/6-31G* Calculations[a]

frequency (intensity)		
17.9(0.52), 31.5(1.1), 40.6(0.7), 63.9(1.3), 70.9(4.6), 118(4.8), 126(1.0), 134(5.8), 149(1.2), 195(34), 224(0.35), 231(0.28), 250(1.9), 263(11), 418(0.9), 423(14), 558(15), 602(20), 640(3.2), 653(6.4), 834(4.8), 836(5.6), 870(0.003), 878(4.8), 1010(9.6), 1022(2.9), 1063(12), 1069(11), 1079(10), 1080(19), 1204(27), 1213(15), 1227(37), 1228(54), 1231(16), 1340(53), 1355(18), 1391(4.3), 1410(25), 1456(20), 1483(15), 1542(83), 1555(24),1561(21), 1564(5.3), 1579(42), 1597(33), 1605(14), 1613(11), 1630(12), 1631(9), 1638(10), 1641(10), 1646(165), 1653(14), 1658(112), 1810(380), 1916(583), 3033(3151), 3209(3.7), 3215(0.05), 3223(19), 3233(12), 3239(10), 3261(1.6), 3278(1.3), 3283(2.3), 3290(0.4), 3299(37), 3304(12), 3308(15), 3323(3.5), 3327(8), 3339(6.2), 3353(0.6)		
rotational constants		
0.064	0.018	0.016

[a] Frequencies and rotational constants in cm^{-1}, intensities in km/mole. Frequencies given here are unscaled but were scaled downward by 0.89 for use in the kinetics calculations.

TABLE 4: Complex-Ion Vibrational Frequencies, Intensities, and Rotational Constants for $(CD_3COCD_3)_2D^+$, MP2/6-31G* Calculations[a]

frequency (intensity)		
26.3(3.7), 46.4(3.7), 48.7(1.5), 53.8(0.28), 70.1(0.16), 74.9(0.47), 84.3(0.04), 134(15), 159(0.48), 214(161), 334(21), 347(28), 414(1.9), 419(0.19), 478(40), 556(293), 684(7.2), 701(4.9), 748(76), 751(2.7), 766(1.4), 770(34), 894(225), 935(31), 941(37), 1013(2.1), 1015(22), 1041(41), 1069(17), 1078(43), 1080(48), 1085(137), 1089(21), 1092(17), 1095(3.7), 1100(40), 1105(48), 1111(718), 1162(31), 1174(64), 1249(1322), 1363(107), 1421(543), 1693(276), 1748(33), 2234(14), 2236(4.6), 2239(4.2), 2240(3.5), 2357(0.25), 2360(0.07), 2361(5.2), 2366(1.4), 2402(0.73), 2412(0.11), 2412(2.1), 2415(2.7)		
rotational constants		
0.112	0.021	0.018

[a] Frequencies and rotational constants in cm^{-1}, intensities in km/mole. Frequencies given here are unscaled but were scaled downward by 0.95 for use in the kinetics calculations.

individual modes are strongly changed by this correlation correction (see Table 4). Previous comparisons between HF and MP2 mode intensities suggested that kinetic modeling of association rates using HF-level ab initio values was nearly as reliable as MP2-level modeling,[13] but the present results for the acetone/protonated acetone complex are not as favorable. For this reaction, the association rates calculated using HF intensities were a factor of 3 lower than those using MP2-corrected values,[31] giving a corresponding difference in modeled binding energy of 1.6 kcal mol^{-1}.

The other part of the k_{ra} calculation is the kinetics of formation and redissociation of the complex A^+B^*. The kinetics are treated by a VTST-based approach incorporating convolutions over a thermal distribution of energies and angular momenta for the reactants. The expression for the association rate constant k_2 (which gives k_{ra} in the zero-pressure limit) is the following:

$$k_2 = \frac{1}{h Q_{\text{reactants}}} \int\int \mathrm{d}E\, \mathrm{d}J N_{EJ} \exp(-E/kT) \times \left\{ \frac{k_r(E,J) + k_c(E,J)[\mathrm{M}]}{k_b(E,J) + k_r(E,J) + k_c(E,J)[\mathrm{M}]} \right\} \quad (5)$$

where $Q_{\text{reactants}}$ is the canonical partition function for separated reactants, and N_{EJ} is the transition state number of states. It has been noted by numerous workers (for example, refs 1, 13, and 32) that in the low-efficiency limit ($k_r \ll k_b$) this expression simplifies so that the properties of the transition state drop out and transition-state theory is unnecessary in the calculations. However, in the present work several of the cases treated do not fall within this limit, and VTST provides a good framework for making accurate calculations including the effects of the large neutral dipole moments on the rates. (Except for such dipole effects, phase-space theory[33] would be equally satisfactory.)

In our application of eq 5, we make the *strong collision* assumption to obtain k_c and a corresponding *strong radiative relaxation* assumption to obtain k_r. The strong collision assumption, which sets $\beta = 1$ in eq 1, says that each collision with the neutral collider stabilizes the metastable complex A^+B^*. The strong radiative relaxation assumption similarly says that emission of one infrared photon stabilizes the metastable complex. A parallel justification for both of these assumptions in the present applications is based on the idea that the redissociation rate constant k_b is strongly dependent on the excess energy of the metastable complex, that is, its internal energy in excess of that needed for dissociation. This excess energy is only about 3000 cm^{-1} even in the largest cases and highest temperatures considered here, so that removal of internal energy on the order of 1000 cm^{-1} or more will drastically reduce k_b and usually lead to ultimate stabilization of the complex. In the case of collisional relaxation, neutral colliders as large and complex as those used here are expected to remove a large fraction of the total internal energy (see ref 34 for an example), so that the $\beta = 1$ assumption seems amply justified. In the case of radiative stabilization, the most likely emitted photon energies are typically of the order of[35] 1000 cm^{-1}; in the butanone/protonated butanone system of greatest concern here, most emitted photons have energies around 1600 cm^{-1}, so that the strong radiative relaxation assumption is considered reasonable for the systems treated here. For larger systems where the excess energy is much larger than 1000 cm^{-1} or for cases with $\beta < 1$, these assumptions will break down, and a master equation treatment will be necessary (as was done by Barker, for instance, to treat collisional relaxation[5]).

The collisional rate constant k_c was calculated by the trajectory-based approach of Su and Chesnavich.[25] For the acetone/protonated acetone system, the assumed value of the binding energy was 30.6 kcal mol^{-1} (in agreement with the recent experimental value[21] of of 30.6). The same value was used for the butanone/protonated butanone system since experimentally this system has the same binding energy as the acetone system.[21] For the acetone-d_6/deuteronated acetone-d_6 system, a binding energy of 29.9 kcal mol^{-1} was used to give the best fit to the room-temperature data point.

Results and Discussion

The systems studied here showed simple association behavior, with straightforward first-order kinetics and no significant

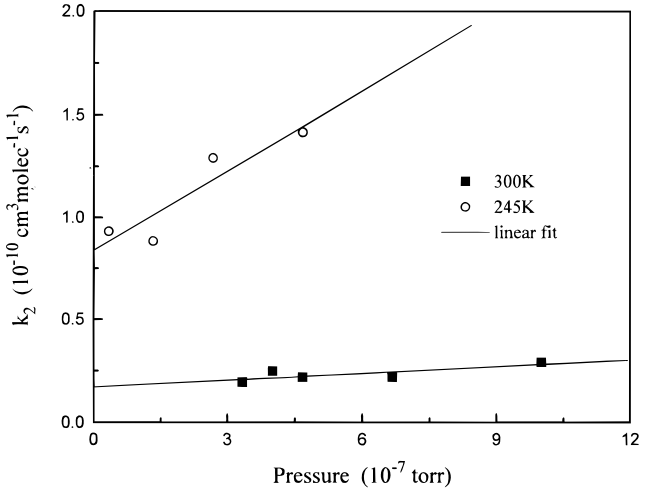

Figure 1. Pressure dependence of the association rate constant for the formation of acetone-d_6 deuteronated dimer at 245 K (open circles) and room temperature (solid squares). The intercepts give $k_{ra} = 8.4 \times 10^{-11}$ cm^3 molecule^{-1} s^{-1} at 245 K and 1.75×10^{-11} cm^3 molecule^{-1} s^{-1} at 300 K.

TABLE 5: Experimental Results and VTST Predictions for the Association of Protonated Acetone with Acetone

T (K)	Φ (exptl)[a]	k_{ra} (exptl)[b]	k_{ra} (VTST)[b]	comment (exptl data)
245	0.016	4.1	4.1	this work
300	0.0046	1.15	1.15	this work
	0.0046	1.16		ref 18
	0.0045	1.13		ref 19
320	0.0030	0.75	0.72	ref 18
330	0.0018	0.47	0.57	ref 19
360	0.0010	0.26	0.30	ref 19
390	0.00076	0.19	0.15	ref 19
420	0.00033	0.083	0.077	ref 19

[a] Collisional efficiency of radiative association, equal to k_{ra}/k_f. [b] 10^{-11} cm^3 molecule^{-1} s^{-1}.

competing reaction processes. The only exception was the NO^+/3-pentanone system where competitive charge transfer occurred, as was previously described.[16,36] A procedure for analyzing the kinetics in this competing-reactions case was discussed in ref 20.

A bimolecular association rate constant k_2 is derived by fitting pseudo-first-order kinetics to a timeplot. This was done for several pressures of the neutral in each system for each temperature. Radiative association rate constants were taken as intercepts of the pressure dependence of association rates (see Figure 1 for example). A useful quantity for making comparisons between different systems is the association efficiency $\Phi = k_{ra}/k_f$. For very fast reactions, Φ levels off toward unity, as association approaches the collisional limit.

Acetone/Protonated Acetone. Experimental results for the formation of the protonated dimer of acetone are given in Table 5 and in Figure 2. As expected, the rate of association decreases rapidly with temperature. The association efficiency is about 2% at 245 K and 0.03% at 420 K.

Acetone-d_6/Deuteronated Acetone-d_6. Experimental results for the formation of acetone-d_6 deuteronated dimer are given in Table 6. While the data are not as extensive as the data for the acetone case, the decrease in association efficiency with increasing temperature is similar, the reaction slowing down by a factor of 5 from 245 to 320 K.

Butanone/Protonated Butanone. The experimental data for the formation of butanone protonated dimer are given in Table 7. This reaction is substantially more efficient at room temperature compared to that of the acetone case due to the larger size of the system. However, the temperature dependences in both systems are quite similar; the rate in the butanone system decreases by a factor of 5 from 300 to 350K, while in the acetone system the corresponding decrease is by a factor of 4.

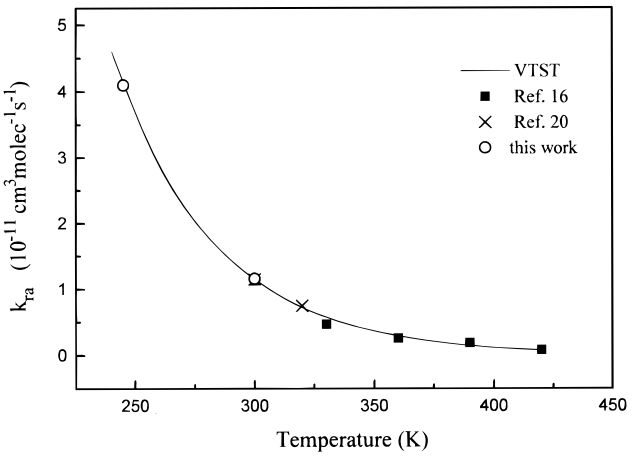

Figure 2. Temperature dependence of the radiative association rate constant for the formation of acetone protonated dimer. Circles represent this work, crosses represent data from ref 18, and squares from ref 19.

TABLE 6: Experimental Results and VTST Predictions for the Formation of Acetone-*D6* Deuteronated Dimer

T (K)	Φ (exptl)[a]	k_{ra} (exptl)[b]	k_{ra} (VTST)[b]	comment (exptl data)
245	0.034	8.40	8.83	this work
300	0.0070	1.75	2.27	this work
320	0.0063	1.58	1.38	ref 18

[a] Collisional efficiency of radiative association, equal to k_{ra}/k_f. [b] 10^{-11} cm^3 molecule^{-1} s^{-1}.

TABLE 7: Experimental Results and VTST Predictions for the Formation of Butanone Protonated Dimer

T (K)	Φ (exptl)[a]	k_{ra} (exptl)[b]	k_{ra} (VTST)[b]
300	0.026	5.7	5.0
314	0.017	3.8	3.6
328	0.0095	2.1	2.6
342	0.0068	1.5	1.8
352	0.0054	1.2	1.3

[a] Collisional efficiency of radiative association, equal to k_{ra}/k_f. [b] 10^{-11} cm^3 molecule^{-1} s^{-1}.

IR Frequencies and Intensities. The vibrational frequencies and infrared intensities for acetone/protonated acetone and the deuteronated analogue were calculated by both HF and MP2 methods and were reported previously.[13] The frequencies/intensities for NO^+/pentanone were calculated at the HF level.[20] Herein we calculated the frequencies of butanone and protonated butanone (Table 1), and the frequencies and intensities of the corresponding complex (Table 3) at the HF/6-31G* level. Reported also are the MP2-level frequencies of acetone-d_6 and deuteronated acetone-d_6 (Table 2) and the frequencies and intensities of their adduct (Table 4) which were calculated but not published previously.

Photon Emission Rate Constants. When a pressure dependence of the apparent bimolecular association rate constant is experimentally observed, the slope $[k_3 = k_f k_b k_c/(k_b + k_r)^2]$ and the intercept $[k_{ra} = k_f k_r/(k_b + k_r)]$ can be solved (as McMahon et al. pointed out[2,17]) to give "measured" values of k_r and k_b. Such semiexperimental rate constants when available

provide a good comparison for the calculated numbers although the assignment of single average values to the microscopic rate constants k_f, k_b, and k_r is inherently approximate. For the acetone/protonated acetone system, the pressure dependence of the association rate has been experimentally observed, and a k_r value of 103 s^{-1} derived.[18] Our data yielded a very similar number of 102 s^{-1} at room temperature, while the value calculated entirely ab initio is somewhat higher at 167 s^{-1}.

For the acetone-d_6/deuteronated acetone-d_6 system, McMahon[18] reported a measured value of $k_r = 106$ s^{-1} at 320 K. Our data gave a measured value of $k_r = 109$ s^{-1} at 300 K and 50 s^{-1} at 245 K (derived from Figure 1). (The latter number, however, should be viewed with caution, noting that in the 245 K measurements the scatter of the experimental points was substantial and the pressure measurement was quite uncertain at this temperature. The derivation of the measured k_r from pressure dependence data by the McMahon-type analysis tends to magnify such uncertainties.) The ab initio-calculated k_r value is about 87 s^{-1} at 300 K and does not change much with temperature.

A weak pressure dependence was observed for the association of butanone with protonated butanone,[20] permitting a McMahon-type analysis to derive a measured k_r value of 36 ± 15 s^{-1} at 300 K. It is surprising that the photon emission rate is so much lower than that for the acetone system. Some reduction, amounting to about 30−40%, is expected in going from acetone to butanone, first because the larger heat capacity of the butanone system means a lower internal temperature of the radiating complex and second because the additional vibrational modes of the butanone system are weak emitters and do not contribute much to the emission. Judging from comparative calculations at the Hartree−Fock level, the emitting frequencies and radiative intensities are quite similar for the acetone and the butanone system. The combination of these factors means that the butanone system has virtually the same set of infrared radiators, but being cooler, they emit photons at a lower rate. Thus, k_r for the butanone system would be expected to be about 60−70% of the acetone value or about 65 s^{-1}. The measured 36 ± 15 s^{-1} is lower than this but not by a disturbing amount. Another similar example can be noted in which a modest size increase in a complex by methyl homologation resulted in an unexpectedly large reduction in k_r: Fisher and McMahon[2] measured the association rate of dimethyl ether with protonated dimethyl ether and derived a k_r value of 48s^{-1}, while a similar determination for diethyl ether with its protonated species gave a k_r of only 18 s^{-1}.

Slopes of log k_{ra} vs T Plots. Previous studies have found that the logarithm of the radiative association rate constant (or efficiency) is linear vs T to good accuracy[13,16,19] although no system has yet been studied with sufficient accuracy over a wide enough temperature range to show that this functional form is superior to other simple alternatives (see ref 19). Our experimental and calculated data for all systems display such a linear dependence (Figure 3). The slopes of these plots should depend strongly on the size of the system. Larger systems are expected to have stronger temperature dependence. The strength of the temperature dependence is, in general, a complex question, but some simplification and insight is possible by considering the low-efficiency limit of association kinetics. For this limiting situation, the equation for the slope taken from ref 13 is

$$\frac{\mathrm{d} \ln k_{ra}}{\mathrm{d}T} = -\frac{n}{T} - \frac{\mathrm{d} \ln Q_{react,vib}}{\mathrm{d}T} \qquad (6)$$

where n is $^1/_2$ of the number of the rotational degrees of freedom for the reactants and $Q_{react,vib}$ is the vibrational partition function

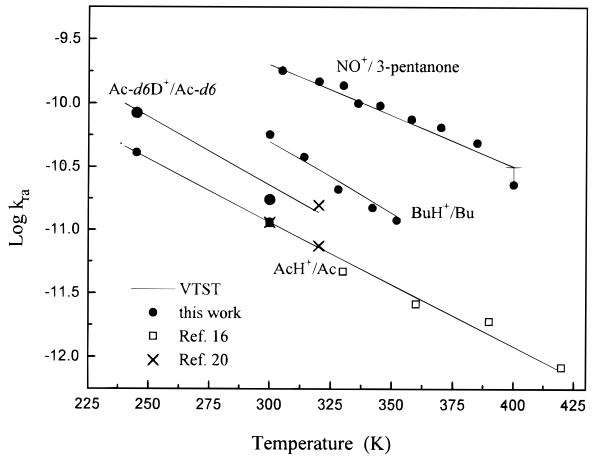

Figure 3. Temperature dependence of the radiative association rates on a semilogarithmic scale. Circles represent data from this work, crosses from ref 18, and squares from ref 19. Lines are VTST calculations. Units of k_{ra} are cm^3 $molecule^{-1}$ s^{-1}.

of the reactants. It was shown[13] for the NO^+/pentanone system that the vibrational contribution to the slope starts to exceed the rotational contribution above ∼120 K, leading to the situation that the rotational contribution to the slope is small near room temperature. The vibrational contribution to the slope in eq 6 is dominant in the 200−500 K range and turns out to be nearly constant with respect to temperature over this range.

Two important conclusions can be drawn from eq 6 (at least within the domain of validity of the low-efficiency approximation, discussed in ref 37). First, the slope of temperature dependence on a semilogarithmic scale does not depend on the properties of the complex, such as the binding energy, or on the nature of the transition state but is only a function of the properties of the individual reactants. Second, the vibrational contribution increases when the size of the system increases and so does the magnitude of the slope. The latter point can be qualitatively understood by considering the contribution of the vibrational partition function in eq 6. This can be written as follows:

$$Q_{react,vib} = \prod_{i=1}^{N} q_{vib,i} \cong (q_{vib})^N \qquad (7)$$

where $q_{vib,i}$ is the partition function for mode i, and q_{vib} is an average partition function representing a typical vibrational mode.[38] Then

$$\ln Q_{react,vib} = \sum_{i=1}^{N} \ln q_{vib,i} \cong N \ln q_{vib} \qquad (8)$$

Thus, the vibrational contribution to the slope increases with the number of degrees of freedom N of the reactants. For a similar series of molecules, the slope of the temperature plot should always increase in magnitude with increasing molecule size, and to a first approximation (assuming that the vibrational contribution is dominant and that the average partition function q_{vib} is similar) we can expect the slope of the ln k vs T plot to increase (become more negative) in proportion to the number of degrees of freedom.

The present work does not offer a big variation in the system size for the purpose of testing this expectation. In going from acetone/protonated acetone (51 degrees of freedom for the reactants) to butanone/protonated butanone (69 degrees of freedom), Figure 3 shows a significant increase in the magnitude

of the slope, consistent with the qualitative expectation. The smallest system, NO^+/pentanone (43 reactant degrees of freedom) has the smallest magnitude of slope, as expected both from its smaller size and from its having 1 less degree of rotational freedom of the reactants. Aside from these qualitative considerations, the real confirmation of our valid understanding of the temperature-dependence variations is the fact that the accurately calculated VTST curves in Figure 3 are in excellent agreement with the observed temperature-dependent points. Approximately straight-line behavior in semilogarithmic coordinates around room temperature (and for higher temperatures as well) is expected from the theory for systems large enough for the vibrational partition function to dominate over the rotational partition function,[13] and indeed it is seen in Figure 3 that straight-line fits to the data are satisfactory within experimental error in all cases.

The calculated association rates are given with the experimental numbers in each table. The agreement between experiment and theory is excellent (see Figure 3). The agreement of calculated and observed temperature dependences is the principal result of this study and encourages the hope that the present theoretical and computational tools are capable of excellent results. The agreement between the predicted and the observed values of the absolute rate constants is remarkably good for the acetone and butanone cases since the calculations have no adjustable parameters; these calculations are entirely based on the ab initio quantum results and on the independently measured experimental binding energies. (For NO^+/pentanone, the agreement of the absolute rate constant values is less significant since the assignment of the best binding energy value in this complex was guided in part by fitting to the RA kinetics results.[16] The binding energy of the acetone-d_6/deuteronated acetone-d_6 system was fitted to the data so that the agreement of absolute rate constants in not meaningful in this case.)

The kinetic modeling indicates that the temperature dependence of k_{ra} is only very weakly dependent on the assumed value of the binding energy. As a specific example, the temperature-dependence data for acetone/protonated acetone were fitted assuming various values of binding energy (adjusting the assumed radiative intensities to maintain the fit to the absolute data values). A variation of 6 kcal mol^{-1} (20%) in the assumed value of the binding energy changed the slope of the calculated ln k_{ra} vs T plot by less than 1%, and for this range of variation, the fit to the data (shown in Figure 3 for the accepted value of binding energy) was equally good for all assumed binding energies.

Conclusions

The high-level VTST-based modeling gives excellent agreement with experiment for temperature dependence of radiative association rates in these four systems. The absolute numbers predicted by the model are also close to the experimental data. This gives confidence in applying VTST modeling using ab initio-calculated molecular properties to make temperature corrections in radiative association kinetics when needed as well as for binding energy estimates from RA kinetics. It is worth mentioning that the ab initio part of the calculations was done at a relatively modest level of theory (such as HF 6-31G*), giving hope that such approaches can work well even in substantially larger systems. However, the significant difference between HF- and MP2-derived results for the acetone/protonated acetone case gives a note of caution against putting too much faith in low-level calculations of radiative emission rates.

Acknowledgment. Support is acknowledged from the National Science Foundation and from the donors of the Petroleum Research Fund, administered by the American Chemical Society.

References and Notes

(1) Bates, D. R.; Herbst, E.. In *Rate Coefficients in Astrochemistry*; Millar, T. J., Williams, D. A., Eds.; Kluwer: Dordrecht, The Netherlands 1988; p 17.
(2) Fisher, J. J.; McMahon, T. B. *Int. J. Mass Spectrom. Ion Processes* **1990**, *100*, 701.
(3) Lin, Y.; Ridge, D. P.; Munson, B. *Org. Mass Spectrom.* **1991**, *26*, 550.
(4) Anicich, V. G.; Sen, A. D.; Huntress, W. T., Jr.; McEwan, M. J. *J. Chem. Phys.* **1991**, *94*, 4189.
(5) Barker, J. R. *J. Phys. Chem.* **1992**, *96*, 7361.
(6) Gerlich, D.; Horning, S. *Chem. Rev.* **1992**, *92*, 1509.
(7) Dunbar, R. C.; Uechi, G. T.; Solooki, D.; Tessier, C. A.; Youngs, W.; Asamoto, B. *J. Am. Chem. Soc.* **1993**, *115*, 12477.
(8) Brownsword, R. A.; Sims, I. R.; Smith, I. W. M.; Stewart, D. W. A.; Canosa, A.; Rowe, B. R. *Astrophys. J.* **1997**, *485*, 195.
(9) Dunbar, R. C. Review: Ion-Molecule Radiative Association. In *Current Topics in Ion Chemistry and Physics*; Ng, C. Y., Baer, T., Powis, I., Eds.; Wiley: New York, 1994; Vol. II.
(10) Cheng, Y. W.; Dunbar, R. C. *J. Phys. Chem.* **1995**, *99*, 10802.
(11) Dunbar, R. C. New Approaches to Ion Thermochemistry via Dissociation and Association. In *Advances in Gas-Phase Ion Chemistry*; Babcock, L. M., Adams, N. G., Eds.; JAI Press: Greenwich, CT, 1996; Vol. 2; p 87.
(12) Dunbar, R. C.; Klippenstein, S. J.; Hrušák, J.; Stöckigt, D.; Schwarz, H. *J. Am. Chem. Soc.* **1996**, *118*, 5277.
(13) Klippenstein, S. J.; Yang, Y.-C.; Ryzhov, V.; Dunbar, R. C. *J. Chem. Phys.* **1996**, *104*, 4502.
(14) Lin, C.-Y.; Chen, Q.; Chen, H.; Freiser, B. S. *Int. J. Mass Spectrom. Ion Processes* **1997**, *167/168*, 713.
(15) Lin, C.-Y.; Dunbar, R. C. *Organometallics* **1997**, *16*, 2691.
(16) Ryzhov, V.; Klippenstein, S. J.; Dunbar, R. C. *J. Am. Chem. Soc.* **1996**, *118*, 5462.
(17) Kofel, P.; McMahon, T. B. *J. Phys. Chem.* **1988**, *92*, 6174.
(18) Thölmann, D.; McCormick, A.; McMahon, T. B. *J. Phys. Chem.* **1994**, *98*, 1156.
(19) Lin, Y., Ph.D. Thesis, University of Delaware, 1992.
(20) Ryzhov, V.; Dunbar, R. C. *Int. J. Mass Spectrom. Ion Processes* **1997**, *167/168*, 627−635.
(21) McMahon, T. B.; Hoffman, T. Proceedings of the 44th ASMS Conference on Mass Spectrometry and Allied Topics, Portland, OR, May 12−16, 1996; p 772.
(22) Dunbar, R. C. *Int. J. Mass Spectrom. Ion Processes* **1990**, *100*, 423.
(23) Lin, C.-Y.; Dunbar, R. C. *J. Phys. Chem.* **1996**, *100*, 655.
(24) Faulk, J. D.; Dunbar, R. C. *J. Phys. Chem.* **1994**, *98*, 11727.
(25) Su, T.; Chesnavich, W. J. *J. Chem. Phys.* **1982**, *76*, 5183.
(26) Gilbert, R. G.; Smith, S. C. *Theory of Unimolecular and Recombination Reactions*; Blackwell: Oxford, 1990.
(27) Baer, T.; Hase, W. L. *Unimolecular Reaction Dynamics: Theory and Experiments*; Oxford: New York, 1996.
(28) Stein, S. E.; Rabinovitch, B. S. *J. Chem. Phys.* **1973**, *58*, 2438.
(29) Dunbar, R. C. *J. Chem. Phys.* **1989**, *90*, 7369.
(30) GAUSSIAN 94. Frisch, M. J.; Trucks, G. W.; Schlegel, H. B.; Gill, P. M. W.; Johnson, B. G.; Robb, M. A.; Cheeseman, J. R.; Keith, T. A.; Petersson, G. A.; Montgomery, J. A.; Raghavachari, K.; Al-Laham, M. A.; Zakrzewski, V. G.; Ortiz, J. V.; Foresman, J. B.; Cioslowski, J.; Stefanov, B. B.; Nanyakkara, A.; Challacombe, M.; Peng, C. Y.; Ayala, P. Y.; Chen, W.; Wong, M. W.; Andres, J. L.; Replogle, E. S.; Gomperts, R.; Martin, R. L.; Fox, D. J.; Binkley, J. S.; Defrees, D. J.; Baker, J.; Stewart, J. J. P.; Head-Gordon, M.; Gonzalez, C.; Pople, J. A. Gaussian, Inc.: Pittsburgh, PA, 1995.
(31) Yang, Y.-C., Ph.D. Thesis, Case Western Reserve University, 1996.
(32) Smith, I. W. M. *Astrophys. J.* **1989**, *347*, 282.
(33) Chesnavich, W. J.; Bowers, M. T. *Prog. React. Kinet.* **1982**, *11*, 137.
(34) Ahmed, M. S.; Dunbar, R. C. *J. Am. Chem. Soc.* **1987**, *109*, 3215.
(35) Dunbar, R. C. *Mass Spectrom. Rev.* **1992**, *11*, 309.
(36) Weddle, G. H.; Dunbar, R. C. *Int. J. Mass Spectrom. Ion Processes* **1994**, *134*, 73.
(37) Dunbar, R. C. *Int. J. Mass Spectrom. Ion Processes* **1997**, *160*, 1.
(38) This is certainly a very oversimplified argument, and the quantity q_{vib} has no actual physical significance. Equation 7 more properly expresses the empirical observation that the distribution of vibrational mode frequencies tends to be similar for different size molecules, and since this is true, the vibrational partition function does in fact tend to be exponential in N. This can also be justified, perhaps more convincingly, on the basis of the observed fact that the thermal vibrational internal energy, $E_{vib} = -\mathrm{d} \ln Q_{vib}/\mathrm{d}(1/kT)$, tends to scale linearly with N.